International Journal of Pavement Engineering
Vol. 9, No. 2, April 2008, 115–128

Taylor & Francis
Taylor & Francis Group

Modelling of combined physical–mechanical moisture-induced damage in asphaltic mixes, Part 1: governing processes and formulations

Niki Kringos[a]*, Tom Scarpas[a], Cor Kasbergen[a] and Patrick Selvadurai[b]

[a]*Faculty of Civil Engineering and Geosciences, Delft University of Technology, Delft, The Netherlands;* [b]*Department of Civil Engineering and Applied Mechanics, McGill University, Montreal, Que., Canada*

(Received 18 March 2007; final version received 5 November 2007)

Moisture has for a long time been recognised as a serious contributor to premature degradation of asphaltic pavements. Many studies have been performed to collect, describe and measure the moisture susceptibility of asphaltic mixes. Most of these are aimed at a comparative measure of moisture damage, either via visual observations from field data or laboratory tests or via mechanical tests, which give a so called moisture damage index parameter. The research presented in this paper is part of an ongoing effort at Delft University of Technology, to move away from such comparative or empirical measures of moisture-induced damage and start treating moisture-induced damage in a comprehensive energy based framework. Such a framework would enable realistic predictions and time-assessment of the failure pattern occurring in an asphaltic pavement under the given environmental and traffic loading which could be rutting, cracking, ravelling or any combination or manifestation thereof. The modelling of moisture-induced damage is a complex problem, which involves a coupling between physical and mechanical damage processes. This paper discusses several modes of moisture infiltration into asphaltic mixes and derives the governing equations for their simulations. Moisture diffusion into the mastic film, towards the aggregate–mastic interface and mastic erosion, due to high water pressures caused by the pumping action of traffic loading, are identified as the main moisture-induced damage processes and are implemented in a new finite element program, named RoAM. The paper discusses the necessary model parameters and gives detailed verification of the moisture diffusion and advective transport simulations. In the accompanying paper the developed finite element model is demonstrated via an elaborate parametric study and the fundamental moisture-induced damage parameters are discussed.

Keywords: simulation of water flow; moisture diffusion; moisture-induced damage; asphaltic mixes; finite element modelling

1. Introduction

Moisture has for a long time been recognised as a serious contributor to premature degradation of asphaltic pavements. Many studies have been performed to collect, describe and measure the moisture susceptibility of asphaltic mixes. Most of these are aimed at a comparative measure of moisture damage, either via visual observations from field data or laboratory tests or via mechanical tests, which give a so called moisture damage index parameter. The previous papers give a comprehensive overview of many of these studies and describe today's most commonly used moisture damage tests. The research presented in this paper is part of an ongoing effort at Delft University of Technology to move away from such comparative or empirical measures of moisture-induced damage and start treating moisture-induced damage in a comprehensive energy based framework. Such a framework would enable realistic predictions and time-assessment of the failure pattern occurring in an asphaltic pavement under the given environmental and traffic loading, which could be rutting, cracking, ravelling or any combination or manifestation thereof.

This paper describes the physical and mechanical moisture-induced damage processes, their analytical and finite element formulation and shows the impact of the various controlling parameters on the predicted damage response. The research work is separated into two parts, Part 1 describes the moisture infiltration processes, gives the formulations of the physical moisture-induced damage processes and demonstrates their analytical verification. In Part 2, the developed tools are demonstrated in an extensive parametric study and the effect of the various identified fundamental moisture-induced damage parameters on the resulting damage formation are discussed.

*Corresponding author. Email: n.kringos@tudelft.nl

ISSN 1029-8436 print/ISSN 1477-268X online

DOI: 10.1080/10298430701792185
http://www.informaworld.com

2. Moisture infiltration into asphaltic mixes

Moisture-induced damage in asphaltic mixes is obviously only an issue if moisture is able to penetrate into the mix. For the identification and simulation of the moisture damage inducing processes in asphaltic mixes, it is therefore important to identify the various moisture infiltration modes. First of all, water may enter the mix due to rainfall, which may cause water flow through the connected macro-pores of the asphalt wearing surface, Figure 1(a). This is especially the case for open graded mixes that are designed to have a high permeability. Secondly, stationary moisture may reside in the macro-pores of the mix, either in liquid or vapour form, Figure 1(b). This can, for instance, be caused by residual moisture after rainfall, a wet subgrade under the wearing surface or a humid environment. Finally, moisture may be present inside the aggregates even before construction of the wearing surface, due to inadequate drying procedures of the aggregates, Figure 1(c) (Rice 1958, Stuart 1990, Fwa and Ong 1994, Huber 2005).

In addition to rainfall, fast water flow through the connected macro-pores of the asphalt mix may also result locally from a saturated wearing surface, when subjected to traffic loading. This phenomenon is often referred to as 'pumping action' (Taylor and Khosla 1983, Kiggundu and Roberts 1988, Kandhal 1992, 1994) and shall be discussed in more detail further on in this paper.

From the above possible modes for moisture infiltration into an asphaltic mix, some are more relevant for open graded asphaltic mixes and others are more relevant for densely graded ones. Regardless of the mix composition, asphaltic mixes with moisture will suffer in due time from moisture-induced damage. In practice, this damage exhibits itself as a dislodging process of the aggregates, a process, which has become known as *ravelling* or *stripping* of the asphaltic mix (Lytton 2002). The dislodging of aggregates from an asphalt wearing surface may show either a pronounced *cohesive* (i.e. within the mastic) or a pronounced *adhesive* (i.e. within the aggregate–mastic bond) failure pattern, or a combination thereof, Figure 2.

Once the wearing surface starts to degrade, progressive physical moisture-induced damage, in combination with traffic loading, may lead to even more severe forms of moisture-induced damage, like pothole forming. The ravelling or stripping of an asphaltic wearing surface is a failure pattern which is undoubtedly related to a combined action of mechanical damage and moisture infiltration, where weakening of the mastic film will promote a cohesive failure pattern and weakening of the aggregate–mastic bond will promote a pronounced adhesive failure pattern.

In the following, the processes which results in the weakening of the asphalt components are identified.

2.1 *Weakening of the aggregate–mastic bond*

The properties of the aggregate–mastic bond play a crucial role in the performance of asphaltic mixes. The reason that asphalt mixes do not qualify as 'unbound granular materials' is the presence of the mastic component, which serves as the binding 'glue' that holds the aggregate matrix together under loading. Essential in this is the *adhesion* of the mastic to the surface of the aggregates. An asphaltic mix which consists of a mastic–aggregate combination which has 'bad adhesion' will have bad mechanical performance and will undoubtedly show a pronounced adhesive failure pattern.

It is known that mastic–aggregate adhesion improves with an increased aggregate surface roughness, Figure 3(a). Clearly, more surface area to adhere to will create a better bond, since the transferred loads will be spread over a larger area. Since mastic is mixed with the aggregates while it is in liquid form, an increased aggregate surface roughness will maximise the mechanical interlock between the mastic and the aggregates, due to the ability of mastic to flow into the surface pores of the aggregates while in liquid form, thus creating mastic 'fingers' inside of the aggregate surface when it solidifies (Figure 3(b)). Such mastic fingers greatly improve the strength of the mastic–aggregate bond, since it requires additional forces to 'unlock' them from the aggregate. However, the interlocking phenomenon relies on the ability of the mastic to come into close contact to the aggregate surface. An asphalt mix which has a mastic component that is not able to spread properly on the aggregate surface, will not benefit from the increased

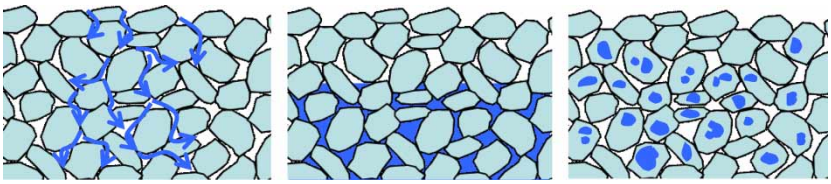

Figure 1. Moisture penetration into the asphalt mix. Available in colour online.

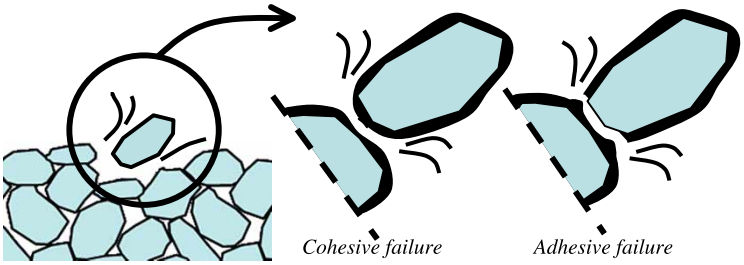

Figure 2. Cohesive vs. adhesive dislodging of an aggregate from the mix. Available in colour online.

adhesive bond, as described above, since it will not be able to fill some of the surface pores, Figure 3(c). The 'spreading capacity' of mastic on an aggregate surface is often referred to as the 'wetting' capacity of the mastic, and can be related to the surface energy properties of the components.

Adhesion is often categorised as thermodynamic, chemical or mechanical adhesion. *Thermodynamic adhesion* refers to equilibrium of interfacial forces or energies, work of adhesion and wetting, *chemical adhesion* refers to adhesion involving chemical bonding at the interface and *mechanical adhesion* arises from the mechanical interlocking over substantial portions of the interface. Despite the various definitions for adhesion, none seem to be completely satisfactory or generally accepted. However, a satisfactory definition for the adhesion of a mastic film on an aggregate surface should somehow account for the thermodynamical as well as the physio-chemical and mechanical aspects of adhesion. Nevertheless, the physio-chemical phenomena which contribute to the adhesion of two materials will, and should, manifest themselves into the mechanical bond properties, which are measurable. The behaviour of the mastic–aggregate interface can therefore be modelled, based on thermodynamically sound relationships in which the physio-chemistry is controlled by internal state variables.

Having moisture in either a stationary or a moving fashion inside of the macro-pores of the asphalt mix, does not explain directly the weakening of the aggregate–mastic bond. Clearly, for the interface to be weakened, moisture must first be able to reach it. Disregarding, for the time being, the possibility of moisture being present in the aggregates itself, and assuming a continuous mastic film without any cracks, moisture can only reach the aggregate–mastic interface by moving through the mastic film. Since mastic has a negligible porosity, the only physical process which explains moisture infiltration into the mastic is molecular diffusion (Thunqvist 2001, Cheng *et al.* 2002, 2003, Masad *et al.* 2005).

When a mastic film is exposed to a stationary moisture field, initially the mastic film and the aggregate–mastic interface have zero moisture content. Then, moisture gradually starts infiltrating through the mastic film, because of the moisture concentration gradient difference inside the mastic. Depending on the moisture diffusion coefficients of the mastic and on the thickness of the mastic film, moisture will eventually reach the aggregate–mastic interface. Common sense indicates that one molecule of moisture reaching the interface will not cause an abrupt debonding effect. As moisture diffusion through the mastic film continues and the moisture concentration gradient diminishes, a significant amount of moisture will reach the aggregate–mastic interface and shall cause progressive debonding of the mastic from the aggregate, Figure 4. An asphaltic mix with poor moisture diffusion characteristics of the mastic and an aggregate–mastic bond which is sensitive to moisture, shall eventually exhibit a predominantly adhesive failure pattern, when exposed to moisture for long periods.

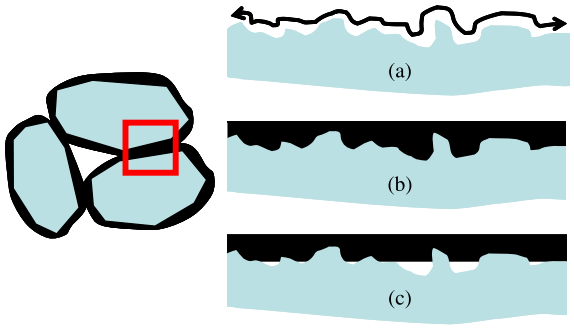

Figure 3. Mastic–aggregate interface surface characteristics (a) rough aggregate surface (b) good mastic wetting and (c) bad mastic wetting. Available in colour online.

2.2 *Weakening of the asphaltic mastic*

The presence of moisture in the pavement may lead to fast water flow through the connecting macro-pores of the asphalt mix. The ongoing action of water flowing past the mastic film may have an erosion effect on the films and cause mastic particles to be removed. This is a physical moisture-induced damage process that continues in the presence high water pressure gradients, and which depends on the desorption characteristics of the

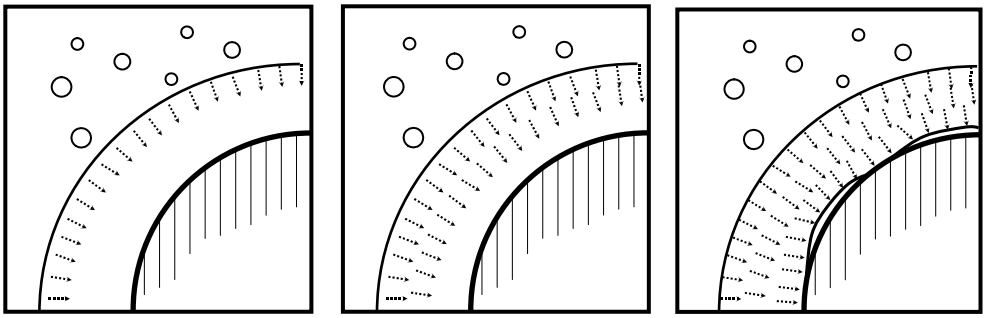

Figure 4. Damage of the mastic–aggregate bond due to moisture infiltration.

mastic. The loss of mastic particles as a consequence of a fast water flow may be referred to as 'washing away', 'scouring' or 'erosion' of the mastic, Figure 5. In this paper this damage process is also referred to as 'advective transport' since this is the approach which is used in this research for its simulation.

As described in the previous section, moisture can infiltrate into the mastic film via molecular diffusion. The building-up of moisture content inside of the mastic may locally cause a weakening of the mastic itself and can actually assist the washing away effect by increasing the desorption characteristics of the mastic, causing an even greater loss of mastic concentration, Figure 6.

In practice, the loss of concentration of mastic means that the asphalt mix is slowly losing the flexibility of its binding component and as such, is becoming weaker and more prone to a cohesive failure pattern, Figure 2(b). In addition to this, thinner mastic films and/or more porous mastic films will promote the movement of moisture towards the aggregate–mastic interface, and therefore contribute also to the loss of the aggregate–mastic bond.

2.3 *Pumping action due to traffic loading*

Another process which is identified in this research as a contributor to moisture-induced damage is the combination of a wet asphaltic mix, exposed to traffic loading. When some of the macro-pores in an asphaltic pavement are saturated, the fast traffic load will locally cause intense water pressure fields in these pores. These excess pore pressures shall even be generated away from the actual wheel path, since the water has no time to redistribute itself within the mix, Figure 7. These pore pressures contribute extra stresses within the asphaltic mix, which may cause added mechanical damage within the asphalt components (Taylor and Khosla 1983, Kiggundu 1988, Kandhal 1992, 1994).

In contrast to the previously described processes, pumping action is categorised in this research as a *mechanical* moisture-induced damage process, since it is directly related to the application of loading to the asphaltic mix. However, this process does have implications for the physical moisture-induced damage processes. For example, the intense pore pressures will locally create a fast water flow field which contributes to the washing away of the mastic particles, which in turn affects the diffusivity characteristics of the mastic. Obviously, mechanical damage of the material, which would also occur under dry circumstances, is included in the model, since the moisture damage is included in an energy-based constitutive framework which can predict elasto-visco-plastic deformations for both the dry and the wet case (Kringos 2007).

2.4 *New approach towards moisture-induced damage*

Clearly, all the above described processes are in reality coupled, and it is their combined effect which results

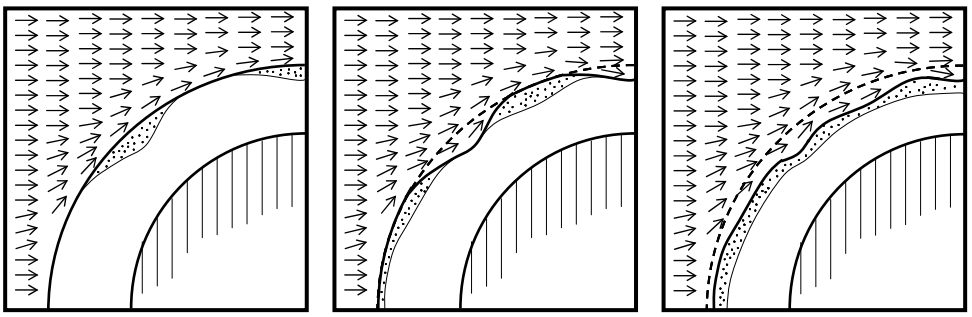

Figure 5. Loss of mastic concentration due to a water flow field.

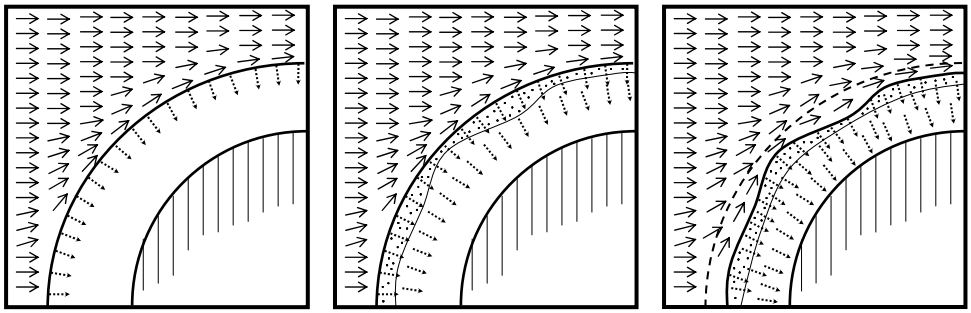

Figure 6. Increased loss of mastic due to weakening of the mastic, caused by moisture diffusion.

in the eventual deformation pattern that the asphalt wearing surface shall exhibit. In summary, in this paper, moisture-induced damage processes are divided into physical and mechanical processes:

The *physical* processes that are included as important contributors to moisture-induced damage are molecular diffusion of moisture, which causes a weakening of the mastic and the aggregate–mastic bond and a 'washing away' or erosion process of the mastic due to high water pressures or a fast flow field. Figure 8(a). The *mechanical* damage process that is identified as a contributor to moisture damage is the occurrence of intense water pressure fields inside the mix caused by traffic loads, which generates additional plastic deformations and is referred to as '*pumping action*'. Obviously, the physical and mechanical processes influence each other and are integrated within a constitutive model for overall moisture–mechanical damage in the mix, Figure 8(b).

Eventually, moisture-induced damage will follow from the combined effect of the physical and mechanical moisture damage inducing processes, which result in a weakening of the mastic and a weakening of the aggregate mastic bond, Figure 8(c).

The above described processes are implemented in a new finite element tool, named ravelling of asphaltic mixes (RoAM) (Kringos and Scarpas 2005, Kringos 2007), which was developed in the Section of Structural Mechanics of Delft University of Technology, as a subsystem of the finite element system CAPA-3D (Scarpas 2000, 2005). The formulations and numerical implementation of the physical moisture-induced damage processes are derived in the following.

3. Simulation of moisture flow in an asphalt mix

Consider a volume v of an asphaltic mix. The mass of the water m present in this volume is

$$m = \int_v \phi S \rho_w \, dv \tag{1}$$

where ρ_w is the water density, ϕ is the effective porosity of the component under consideration and S is the degree of saturation in the component under consideration.

The change of water mass that can take place as a result of net fluid flow out of the volume v across the

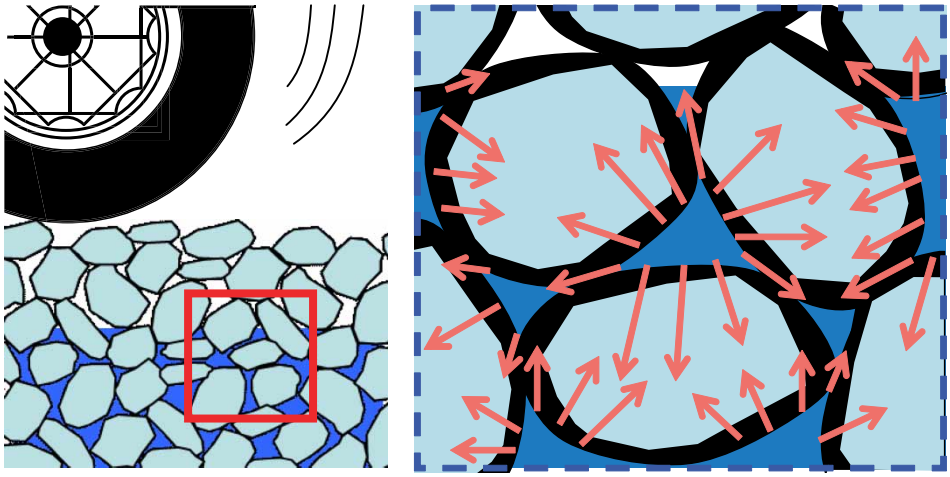

Figure 7. Pumping action on a pavement. Available in colour online.

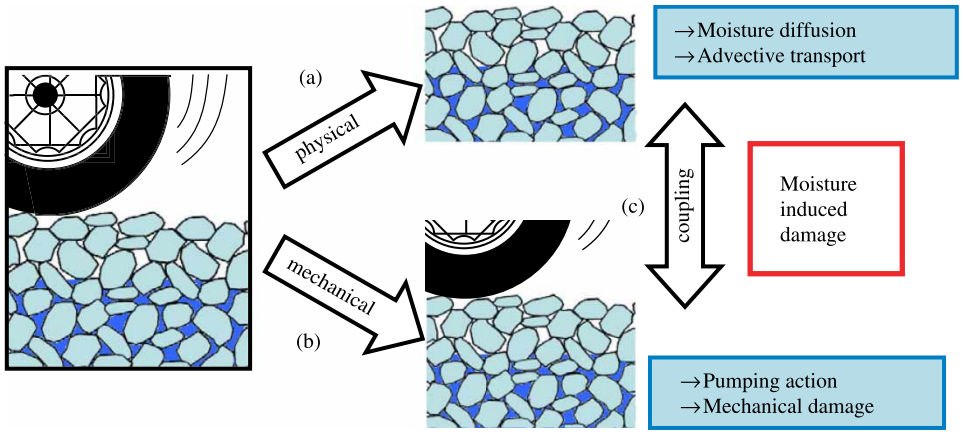

Figure 8. Schematic of the new approach towards moisture-induced damage. Available in colour online.

boundary surface $\partial\Omega$ is described by the net transport of mass flux

$$F_a = \int_{\partial\Omega} \rho_w \underset{\sim}{\mathbf{v}} \cdot \underset{\sim}{\mathbf{n}} \, ds \tag{2}$$

where $\underset{\sim}{\mathbf{v}}$ is the water flow velocity and $\underset{\sim}{\mathbf{n}}$ is the outward unit normal to $\partial\Omega$.

If the water mass is conserved (i.e. neglecting chemical reactions or phase changes), the rate of change in fluid mass in the region is equal to the water flux out of the region

$$\frac{Dm}{Dt} = -F_a \tag{3}$$

Based on the above, the water mass balance can be found as (Kringos 2007):

$$\operatorname{div}\left(\frac{\rho_w g}{\mu} \underset{\approx}{\mathbf{k}} (\nabla h + \nabla z)\right) = L\frac{dh}{dt} \tag{4}$$

whereby, μ is the dynamic viscosity of the water, $\underset{\approx}{\mathbf{k}}$ is the intrinsic permeability tensor, h is the pressure head, z is the datum and L is the storage coefficient.

Using Darcy's law

$$\underset{\sim}{\mathbf{v}} = -\frac{\rho_w g}{\mu} \underset{\approx}{\mathbf{k}} (\nabla h + \nabla z) \tag{5}$$

The governing equation for the water balance in the asphalt components can be simplified to

$$L\frac{dh}{dt} + \operatorname{div}(\underset{\sim}{\mathbf{v}}) = 0 \tag{6}$$

3.1 *Moisture diffusion through the mastic film*

The movement of moisture through the mastic film is considered to be a process that occurs at a molecular level. To simulate the process of moisture diffusion into the components of the asphalt mix, Fick's phenomenological law of diffusion is employed (Fick 1855).

The diffusion flux of moisture $\underset{\sim}{\mathbf{J}}_d$ is defined as

$$\underset{\sim}{\mathbf{J}}_d = -\underset{\approx}{\mathbf{D}} \nabla C_m \tag{7}$$

where C_m is the current moisture concentration in the material. The diffusion of the material is determined by the diffusion tensor $\underset{\approx}{\mathbf{D}}$

$$\underset{\approx}{\mathbf{D}} = \sum_{i,j} D_{ij} \underset{\sim}{\mathbf{e}}_i \otimes \underset{\sim}{\mathbf{e}}_j = a_m \tau \delta_{ij} \tag{8}$$

where a_m is the molecular diffusion coefficient, τ is the tortuosity of the material and δ_{ij} is the Kronecker delta.

Equation (7) assumes that the process of moisture diffusion into the mastic film is solely attributed to mixing on a micro-scale, depending on a spatial gradient of moisture concentration. Posing the conservation of mass principle, it can be found

$$\frac{\partial}{\partial t} C_m = -\operatorname{div}\left(\underset{\sim}{\mathbf{J}}_d\right) = \operatorname{div}\left(\underset{\approx}{\mathbf{D}} \nabla C_m\right) \tag{9}$$

which is also known as Fick's second law.

The moisture content θ within the material is defined as

$$\theta = \frac{C_m}{C_m^{max}} \tag{10}$$

where C_m^{max} is the maximum moisture concentration uptake of the material. The mass of moisture, present in the mastic at time t, is therefore controlled by both the diffusivity $\underset{\approx}{\mathbf{D}}$ and the maximum moisture concentration C_m^{max} uptake in the mastic, Figure 9.

From Figure 9 it can be seen that a material which has a high moisture diffusion coefficient (material β) does

not necessarily have the highest moisture uptake. Even though material α has a lower diffusion coefficient, it eventually absorbs a bigger amount of moisture, due to its higher moisture uptake capacity, ${}^{\alpha}C_{\mathrm{m}}^{\max}$.

Due to the differences in time scales, the mass balance law for water which infiltrates into the asphalt mix via a pressure gradient driven process, as discussed in the previous section, and moisture which infiltrates into the mix via a concentration gradient driven diffusion process, are modelled separately.

3.2 Moisture inducing erosion damage of the mastic film

The mastic film is an important component in asphaltic mixes; it is the 'glue' that keeps the aggregates together. It also gives the visco-elasto-plastic and self-healing characteristic to the asphalt. Damage of the mastic, due to moisture infiltration is modelled in this research via two physical processes. The first is related to a weakening of the mastic due to moisture diffusion and the second is related to an erosion of the mastic, due to traffic-related high water pressures in the macro-pores of the asphalt mix.

In this section, the governing equation for the modelling of erosion of mastic, or loss of mastic concentration, due to water pressure are given.

Considering an asphaltic mix exposed to water, mastic particles can be present in the mix in two different forms: adsorbed or desorbed. Adsorbed mastic particles are still part of the mix and contribute to the overall mix characteristics. Desorbed mastic particles have been separated from the mix and are being transported via the water out of the mix; they are no longer contributing to the mechanical or physical characteristics of the asphalt.

In the following, the mastic that is desorbed from the mix and is no longer contributing to the mechanical strength of the mastic, is shown as the dissolved mastic concentration C_{d}

$$C_{\mathrm{d}} = \frac{\mathrm{m}_{\mathrm{desorbed\_mastic}}}{V_{\mathrm{water}}} \tag{11}$$

The mastic which is still part of the asphalt is shown as the adsorbed mastic content C_{a}

$$C_{\mathrm{a}} = \frac{\rho^{\mathrm{m}}}{\rho_0^{\mathrm{m}}} \tag{12}$$

where ρ_0^{m} is the, undamaged, reference density of the mastic and ρ^{m} is the current density.

Considering the spatial scalar field $C = C(\underset{\sim}{\mathbf{x}}, t)$ that describes the concentration of mastic at time t. Assuming C to be continuously differentiable, the current amount of mastic mass $\mathrm{m}(t)$ in some 3D region Ω with volume v given time t may be characterised by the scalar-valued function

$$\mathrm{m}(t) = \int_{\Omega} C(\underset{\sim}{\mathbf{x}}, t)\mathrm{d}v \tag{13}$$

The concentration mastic at a given place in the asphalt mix can consist of desorbed or adsorbed mastic particles

$$C(\underset{\sim}{\mathbf{x}}, t) = \phi S C_{\mathrm{d}} + \rho_0^{\mathrm{m}} C_{\mathrm{a}} \tag{14}$$

where ϕ is the porosity and S is the degree of saturation at time t at $\underset{\sim}{\mathbf{x}}$.

The change of mastic mass in the volume Ω might take place as a result of an advective and a diffusive flux across the boundary surface $\partial\Omega$.

The advective flux F_{a} is defined as

$$F_{\mathrm{a}} = \int_{\partial\Omega} C_{\mathrm{d}} \underset{\sim}{\mathbf{v}} \cdot \underset{\sim}{\mathbf{n}} \, \mathrm{d}s \tag{15}$$

The diffusive flux F_{d} is defined as

$$F_{\mathrm{d}} = -\int_{\partial\Omega} \underset{\approx}{\mathbf{D}}_{\mathrm{m}} \nabla C_{\mathrm{d}} \cdot \underset{\sim}{\mathbf{n}} \, \mathrm{d}s \tag{16}$$

where $\underset{\approx}{\mathbf{D}}_{\mathrm{m}}$ is the diffusion/dispersion tensor and $\underset{\sim}{\mathbf{n}}$ denotes the outward unit normal acting along the boundary surface $\partial\Omega$

The diffusion/dispersion tensor (Bear, 1972) is depicted as

$$\begin{aligned} \underset{\approx}{\mathbf{D}}_{\mathrm{m}} &= \sum_{i,j} D_{ij} \underset{\sim}{\mathbf{e}}_i \otimes \underset{\sim}{\mathbf{e}}_j \\ &= a_m \tau \theta \delta_{ij} + a_t |\underset{\sim}{\mathbf{v}}| \delta_{ij} + (a_l - a_t) \frac{v_i v_j}{|\underset{\sim}{\mathbf{v}}|} \end{aligned} \tag{17}$$

where a_m is the molecular diffusion coefficient, τ is the tortuosity, a_t is the transverse dispersivity and a_l is the longitudinal dispersivity.

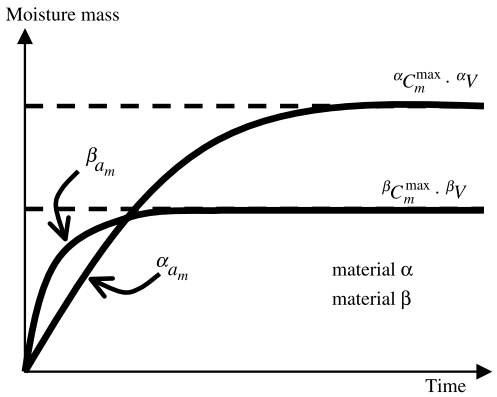

Figure 9. Schematic of moisture diffusion in two different materials.

Similar to the mass balance of moisture, the mastic mass balance can be found as (Kringos 2007):

$$\frac{\partial(\theta C_d + \rho_0^m C_a)}{\partial t} + \mathrm{div}(C_d \underset{\sim}{\mathbf{v}}) - \mathrm{div}(\underset{\sim}{\mathbf{D}}_m \cdot \nabla C_d) = -(\theta C_d + \rho_0^m C_a)\alpha \frac{\partial p}{\partial t} \quad (18)$$

where α is the compressibility coefficient of the material.

The first term of Equation (18) on the LHS represents the change of mass accumulation, the second term represents the net change of mass flux due to advection, the third term is the net mass flux due to dispersion and diffusion and the term on the RHS is the change of mass 'production' due to consolidation of the medium.

The change of mass accumulation term of Equation (18) can be expanded into

$$\frac{\partial(\theta C_d + \rho_0^m C_a)}{\partial t} = \frac{\partial(\theta C_d)}{\partial t} + \frac{\partial(\rho_0^m C_a)}{\partial t} = \theta \frac{\partial C_d}{\partial t} + C_d \frac{\partial \theta}{\partial t} + \rho_0^m \frac{\partial C_a}{\partial t} \quad (19)$$

The advective flux term of Equation (18) can be written as

$$\mathrm{div}(C_d \underset{\sim}{\mathbf{v}}) = C_d \mathrm{div}\, \underset{\sim}{\mathbf{v}} + \underset{\sim}{\mathbf{v}} \nabla C_d \quad (20)$$

From the balance of the fluid mass in Equation (6) the divergence of the velocity field is known

$$\mathrm{div}\, \underset{\sim}{\mathbf{v}} = -L \frac{\partial h}{\partial t} \quad (21)$$

Substituting Equation (21) into the advective flux term Equation (20) yields

$$\mathrm{div}(\underset{\sim}{\mathbf{v}} C_d) = -C_d L \frac{\partial h}{\partial t} + \underset{\sim}{\mathbf{v}} \nabla C_d \quad (22)$$

Substituting Equations (22) and (19) into (18) yields the governing equation of the mastic:

$$\theta \frac{\partial C_d}{\partial t} + \rho_0^m \frac{\partial C_a}{\partial t} + \underset{\sim}{\mathbf{v}} \nabla C_d - \mathrm{div}\left(\underset{\sim}{\mathbf{D}}_m \cdot \nabla C_d\right) = -(\theta C_d + \rho_0^m C_a)\alpha^* \frac{\partial h}{\partial t} + \left(L \frac{\partial h}{\partial t} - \frac{\partial \theta}{\partial t}\right) C_d \quad (23)$$

The relationship between the adsorbed mastic content C_a and the desorbed concentration of mastic C_d can be described via an isotherm. The type of isotherm used in the analysis to define this relationship (e.g. linear, Langmuir, Freundlich) can be based on experimental data and shows the desorption characteristics of the mastic in the presence of a water field. A few examples of isotherms can be found in Figure 10, based on the Langmuir relation

$$C_a = \frac{\alpha C_d}{1 + \beta C_d} \quad (24)$$

where α and β are coefficients of the Langmuir isotherm.

3.3 *Numerical approximation of the flow equation*

The flow equation was derived in Equation (6) and must be reformulated into a more suitable form to be used in the finite element method (Kringos 2007):

$$\sum_{j=1}^{n} \left(\int_V N_i L(h) N_j \mathrm{d}V \right) \frac{\mathrm{d}h_j}{\mathrm{d}t} + \sum_{j=1}^{n} \left(\int_V \nabla N_i \underset{\sim}{\mathbf{K}} \nabla N_j \mathrm{d}V \right) h_j = \int_S N_i \underset{\sim}{\mathbf{K}} (\nabla h + \nabla z) \mathrm{d}S - \int_V \nabla N_i \underset{\sim}{\mathbf{K}} \nabla z \mathrm{d}V \quad (25)$$

whereby N_i are the shape functions of the isoparametric finite elements. Equation (25) can be written in matrix form as

$$[\mathbf{m}] \left\{ \frac{\mathrm{d}h}{\mathrm{d}t} \right\} + [\mathbf{S}]\{h\} = \{\mathbf{B}\} + \{\mathbf{G}\} \quad (26)$$

Reformulation of the flow equation into a summation of matrices allows for the implementation of the numerical approximation of this non-linear equation. These governing equations are implemented in the finite element method.

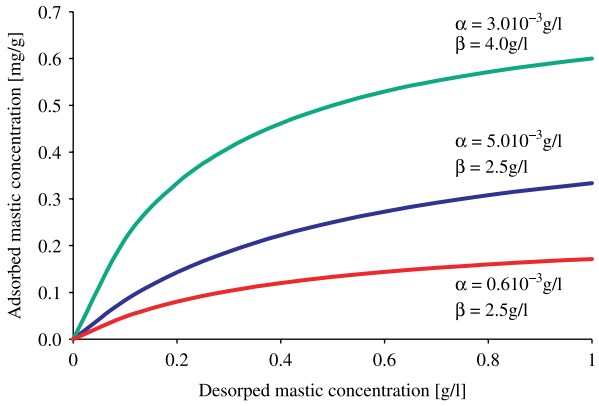

Figure 10. Examples of desorption isotherms, based on the Langmuir relation.

3.4 Numerical approximation of the mastic transport equation

The mastic transport equation as shown in Equation (23) involves two unknowns, the adsorbed C_a and the desorbed C_d mastic particles. In order to solve this equation, a relation between these two quantities must be defined. In addition to the Langmuir relationship, other relationships that can be chosen are, for instance, a linear isotherm

$$C_a = K_d C_d \tag{27}$$

where K_d is the desorption coefficient, or a nonlinear (Freundlich) isotherm

$$C_a = \gamma C_d^n \tag{28}$$

where γ is the Freundlich coefficient and n is a power index (Bear and Bachmat 1990). The choice of the isotherm and the corresponding parameters, should follow from experimental data.

By choosing the *linear* isotherm for the adsorbed–desorbed mastic relation, Equation (25) becomes

$$\begin{aligned}&\left(\theta+\rho_0^m K_d\right)\frac{\partial C_d}{\partial t}+\underset{\sim}{\mathbf{v}}\nabla C_d=\operatorname{div}\left(\underset{\sim}{\mathbf{D}}_m\cdot\nabla C_d\right)\\&-\alpha^*\frac{\partial h}{\partial t}\left(\theta+\rho_0^m K_d\right)C_d+\left(L\frac{\partial h}{\partial t}-\frac{\partial\theta}{\partial t}\right)C_d\end{aligned} \tag{29}$$

Equation (29) describes the transport of mastic from an Eulerian (or fixed) framework for a linear constitutive relation. The combination of advective and dispersive/diffusive terms in the mastic transport equation could cause numerical difficulties. These difficulties have been well documented in the literature and various attempts to handle them have been summarised by many authors (e.g. Neuman 1981, Kinzelbach 1987, Lobo Ferreira 1987, Casulli 1990, Dong and Selvadurai 2006, Selvadurai and Dong 2006a, b).

In RoAM, a Lagrangian–Eulerian method is implemented. Lagrangian–Eulerian methods generally solve the advective part of the problem by a 'method of characteristics' and the diffusive part by Eulerian grid methods, such as finite elements. The traditional 'method of characteristics' is explicit and tracks particles forward in a manner which is computationally intensive. Therefore, in RoAM a modified method is used which is implicit and has good numerical stability. In this method the path lines of the particles are traced backwards according to a single step reverse algorithm (Neuman 1981, Douglas and Russel 1982, Baptista *et al.* 1984, Casulli 1987). More details of the formulation can be found in Kringos (2007).

The finite element approximation of the governing mastic equation (Equation (23); with a linear isotherm) becomes

$$\begin{aligned}&\sum_{j=1}^{n}\left(\int_V N_i(\theta+\rho_0^m K_d)N_j\mathrm{d}V\right)\frac{DC_j^d}{Dt}\\&+\sum_{j=1}^{n}\left(\int_V(\nabla N_i\underset{\sim}{\mathbf{D}}_m\cdot\nabla N_j)\mathrm{d}V\right)C_j^d\\&+\sum_{j=1}^{n}\left(\int_V N_i\alpha^*\frac{\partial h}{\partial t}(\theta+\rho_0^m K_d)N_j\mathrm{d}V\right)C_j^d\\&-\sum_{j=1}^{n}\left(\int_V N_i\left(L\frac{\partial h}{\partial t}-\frac{\partial\theta}{\partial t}\right)N_j\mathrm{d}V\right)C_j^d\\&=\int_S\underset{\sim}{\mathbf{n}}N_i\underset{\sim}{\mathbf{D}}_m\cdot\nabla C_d\mathrm{d}S\end{aligned} \tag{30}$$

Since the storage term L is multiplied by the rate of the hydraulic head in Equation (30), the partial derivative of the moisture content w.r.t. the hydraulic head becomes the rate of moisture content

$$L\frac{\partial h}{\partial t}=\left(\alpha^*\frac{\theta}{\phi}+\phi\frac{\partial S}{\partial h}\right)\frac{\partial h}{\partial t}=\alpha^*\frac{\theta}{\phi}\frac{\partial h}{\partial t}+\frac{\partial\theta}{\partial t} \tag{31}$$

Substituting Equation (31) into (30), gives

$$\begin{aligned}&\sum_{j=1}^{n}\left(\int_V N_i(\theta+\rho_0^m K_d)N_j\mathrm{d}V\right)\frac{DC_j^d}{Dt}\\&+\sum_{j=1}^{n}\left(\int_V(\nabla N_i\underset{\sim}{\mathbf{D}}_m\cdot\nabla N_j)\mathrm{d}V\right)C_j^d\\&+\sum_{j=1}^{n}\left(\int_V N_i\alpha^*\frac{\partial h}{\partial t}(\theta+\rho_0^m K_d)N_j\mathrm{d}V\right)C_j^d\\&-\sum_{j=1}^{n}\left(\int_V N_i\left(\alpha^*\frac{\theta}{\phi}\frac{\partial h}{\partial t}\right)N_j\mathrm{d}V\right)C_j^d\\&=\int_S N_i\underset{\sim}{\mathbf{n}}\cdot\underset{\sim}{\mathbf{D}}_m\cdot\nabla C_d\mathrm{d}S\end{aligned} \tag{32}$$

Equation (32) can be written in the following matrix format

$$[\mathbf{m}]\left\{\frac{DC_d}{Dt}\right\}+([\mathbf{D}]+[\mathbf{K}])\{C_d\}=\{\mathbf{Q}\}+\{\mathbf{B}\} \tag{33}$$

where either a concentration or a concentration flux can be given as boundary conditions.

4. Comparison to closed form solutions

In the previous sections the governing equations of the physical moisture-induced damage processes and their finite element formulation are given. In the following a few benchmarks are performed to verify the correctness of the implemented equations. In the following, diffusion and advective transport simulations with RoAM are compared to closed form solutions.

4.1 Diffusion equation

General solutions of the diffusion equation can be obtained for a variety of initial and boundary conditions provided the diffusion coefficient is constant. Such a solution usually has one of two standard forms. Either it comprises a series of error functions or related integrals or it is in the form of a trigonometric series. In the following, comparisons are made between the results of RoAM and the analytical solution for diffusion into a semi-infinite medium and a hollow sphere.

4.1.1 Validation 1

An example of a linear diffusion problem that may be solved using an error function is that of a 1D diffusion into a semi-infinite medium with an initial overall concentration $C_0 = 0$ and a constant left boundary condition C_t (Crank 1975, Selvadurai 2000). The concentration field can be found as

$$C(x,t) = C_t \operatorname{erfc}\left(\frac{x}{2\sqrt{Dt}}\right) \tag{34}$$

where the function erfc(y) can be found from the error function erf(y), defined as

$$\operatorname{erfc}(y) = 1 - \operatorname{erf}(y) = 1 - \frac{2}{\sqrt{\pi}}\int_0^y \mathrm{e}^{-\eta^2}\,\mathrm{d}\eta \tag{35}$$

The above solution is used to verify the finite element results of the diffusion algorithm of RoAM. For the simulation, a diffusivity $D_x = 1.0\,\mathrm{mm}^2/\mathrm{h}$, a total length of the mesh $l_x = 100\,\mathrm{mm}$ and 200 elements were used (i.e. $\Delta x = 0.5\,\mathrm{mm}$). A comparison of the normalised concentration values $C(10, t)/C_t$ is shown in Figure 11. A good comparison is found. A sensitivity study with respect to the mesh discretisation showed that a mesh discretisation of 100 and 10 elements give comparable results.

4.1.2 Validation 2

For the second validation of the diffusion algorithm, the problem of diffusion into a hollow sphere is chosen. In the outset, this example could be related to an aggregate coated in a bituminous mastic film, which is exposed to a wet environment. The hollow sphere under consideration has a thickness of $t = r_2 - r_1$, with the outside surface r_2 and the inner surface r_1, Figure 12.

If the inside and the outside surfaces are maintained at a constant concentration of C_1 and C_2, respectively and the region $r_1 \le r \le r_2$ is initially at C_0, the concentration approaches the steady-state distribution according to the expression (Carslaw and Jaeger 1959)

$$C = \frac{r_1 C_1}{r} + \frac{(r_2 C_2 - r_1 C_1)(r - r_1)}{r(r_2 - r_1)} + \frac{2}{r\pi}\sum_{n=1}^{\infty}\frac{r_2(C_2 - C_0)\cos n\pi - r_1(C_1 - C_0)}{n}\Bigg] \cdot \sin\frac{n\pi(r - r_1)}{r_2 - r_1}\exp\left[\frac{-Dn^2\pi^2 t}{(r_2 - r_1)^2}\right] \tag{36}$$

For the comparison of this solution with the RoAM simulation, an analysis is made with diffusivity $D_r = 0.01\,\mathrm{mm}^2/\mathrm{h}$, a radius of the outside service of $r_2 = 200\,\mathrm{mm}$ and a film thickness $t = 14\,\mathrm{mm}$. The finite element mesh is divided in 7 layers of equal thickness, i.e. $\Delta r = 2\,\mathrm{mm}$. The inside concentration is kept at $C_1 = 0.0$ and an initial concentration of $C_0 = 0.0$ is utilised.

The normalised concentration values $C = C(r_{\mathrm{node}}, t)/C_2$ for three nodes in different layers in the mesh are compared to the analytical solution, Figure 13. A good comparison is found.

4.2 Advective transport

The accurate computational modelling of an advection–diffusion transport equation, especially in the presence of an advection-dominated term, with either a discontinuity or steep gradient of the dependent variable, has been addressed to varying degrees of success in the field of

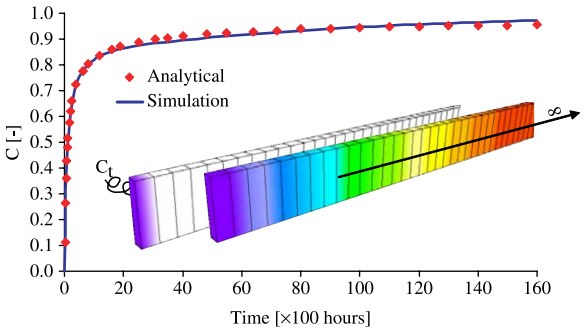

Figure 11. Comparison of analytical solution with RoAM simulation. Available in colour online.

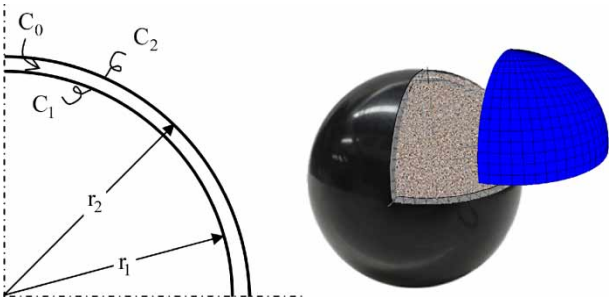

Figure 12. One dimensional diffusion into a hollow sphere. Available in colour online.

computational fluid dynamics (LeVeque 1992, Morton 1996, Quarteroni and Valli 1997, Ganzha and Vorozhtsov 1998, Wang and Hutter 2001, Atluri 2004, Selvadurai and Dong 2006, 2007). Higher-order methods require the size of the domain discretisation element to be small enough, such that the elemental Péclet number should not be greater than unity.

When the elemental Péclet number is greater than unity the methods give rise to unrealistic numerical phenomena such as oscillations, negative concentrations and artificial diffusion at regions close to a leading edge with a discontinuous front. For this reason, in conventional higher-order methods for advection dominated problems, a finer mesh is invariably used throughout the region, since the velocity field is usually not known *a priori*. This places a great demand on computational resources, particularly in simulations involving 3D problems. The first order methods such as the Lax–Friedrich scheme, on the other hand, eliminate the oscillatory behaviour at discontinuous fronts, where there is no physical diffusion (i.e. $Pe = \infty$), but give rise to numerical dispersion in the solution. This feature is generally accepted for purpose of the engineering usage of the procedures, but from a computational point of view gives rise to strong reservations concerning the validity of the procedures developed for the advection–diffusion transport equation for the solution of the purely advective transport problem.

Furthermore, if physical diffusive phenomena are present in the transport problem, it becomes unclear as to whether the diffusive patterns observed in the solution are due to the physical process or an artefact of the numerical scheme.

Evaluating the accuracy of the purely advective transport problem is therefore a necessary pre-requisite to gaining confidence in the application of the computational scheme to the study of the advection–diffusion problem. The real test for a computational scheme developed for modelling the advection dominated transport problem is to establish how accurately the computational scheme can converge to the purely advective transport problem at zero physical diffusion

The validation of the presented numerical approach in RoAM is made by comparing the computational results with two 1D exact closed form solutions involving the advective transport problem.

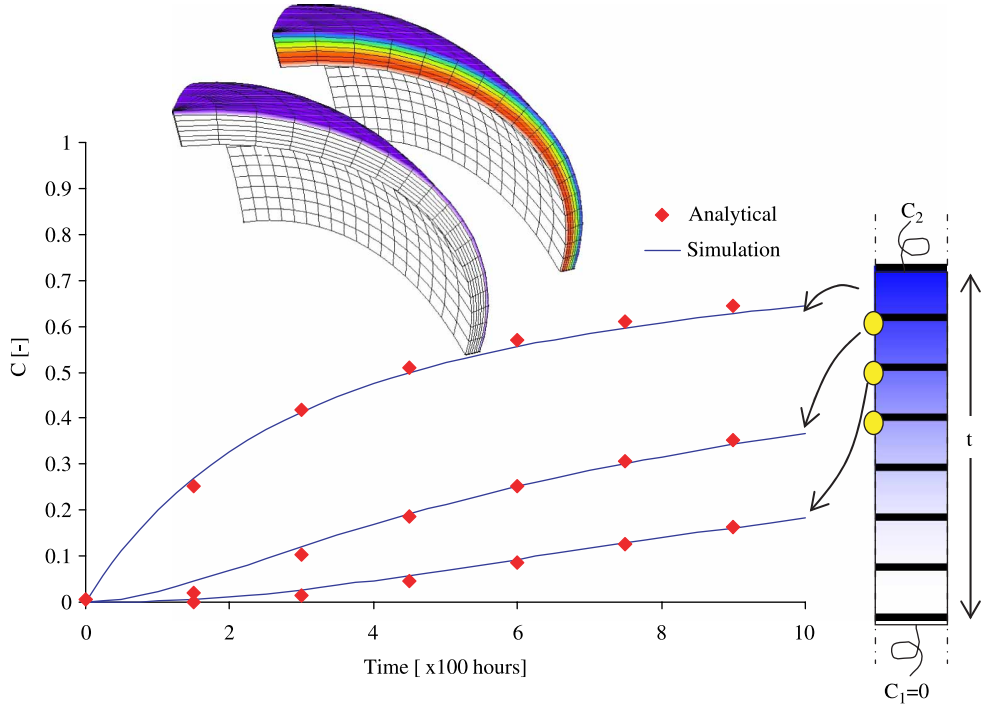

Figure 13. Comparison analytical solution and RoAM simulation. Available in colour online.

4.2.1 Validation 1

For the first validation, a finite element mesh of length $L_x = 10\,\text{mm}$ with negligible y and z dimensions is exposed to a water flow field of constant velocities $v_x = v_0$ and $v_y = v_z = 0.0\,\text{mm/s}$. The region is assumed fully saturated and the diffusion tensor $\mathbf{D}_\text{m}$ is zero. At time $t = 0.0\,\text{s}$ the region is subjected to a discontinuous desorbed mastic concentration front at the boundary in the form of a Heaviside step function $H(t)$.

These conditions reduce the mastic transport equation to a one dimensional purely advective transport equation of the form

$$\frac{\partial C_\text{d}}{\partial t} + v_0 \nabla C_\text{d} = 0 \tag{37}$$

with the boundary conditions

$$C_\text{d}(0,t) = C_0 H(t) \quad C_\text{d}(x,0) = 0.0 \tag{38}$$

The exact analytical development of the desorbed mastic concentration field is, in this case, given by Selvadurai and Dong (2006). In Figure 14 the numerical solutions for $v_0 = 1.0\,\text{mm/s}$ and $C_0 = 1.0$ at $x = 10.0\,\text{mm}$ are compared to the exact analytical solution for various mesh refinements, whereby using a constant Courant number, Cr, equal to 1.0

$$Cr = \frac{|v_x|\text{d}t}{h_x} \tag{39}$$

where dt is the time step and h_x is the element size.

It can be seen from Figure 14 that with increased mesh refinement, the numerical diffusion is reduced and the concentration front is simulated quite accurately without oscillatory effects. It may be observed that none of the discretisations exhibit any numerical oscillation.

4.2.2 Validation 2

For the second validation, the same finite element mesh is exposed to a changing flow field of

$$v_x = v_0 \exp(-\lambda t) \tag{40}$$

and $v_y = v_z = 0.0\,\text{mm/s}$. The region is assumed fully saturated with negligible water capacity $\tilde{\theta}$ and a zero diffusion tensor, $\mathbf{D}_\text{m}$. At time $t = 0.0\,\text{s}$ the same boundary conditions as in the first validation are assumed, Equation (38).

These conditions simplify the mastic transport equation to the form

$$\frac{\partial C_\text{d}}{\partial t} + v_0 \exp(-\lambda t) \nabla C_\text{d} = 0 \tag{41}$$

and the developing desorbed mastic concentration field under these conditions can be found analytically as (Selvadurai and Dong 2006)

$$C_\text{d}(x,t) = C_0 H \left[\frac{\left[1 - \exp(-\lambda t)\right]}{\lambda} - \frac{x}{v_0} \right] \tag{42}$$

Because the velocity field is time dependent, the Courant number is not constant either and can be found from

$$Cr = \beta \text{e}^{-0.02t} \tag{43}$$

In Figure 15 the numerical solutions at $x = 10.0\,\text{mm}$ with $v_0 = 1.0\,\text{mm/s}$, $C_0 = 1.0$, $\beta = 1.0$ and $\lambda = 0.02\,s^{-1}$ are compared to the analytical solution Equation (42) for various mesh refinements. It can be seen that, for the case under consideration, an increased refinement of 500 elements, with $h_x = 0.02\,\text{mm}$ and $\text{d}t = 0.02\,s$, approximates the analytical solution with negligible numerical dispersion. Again, none of the discretisations showed any signs of numerical oscillations in the approximation.

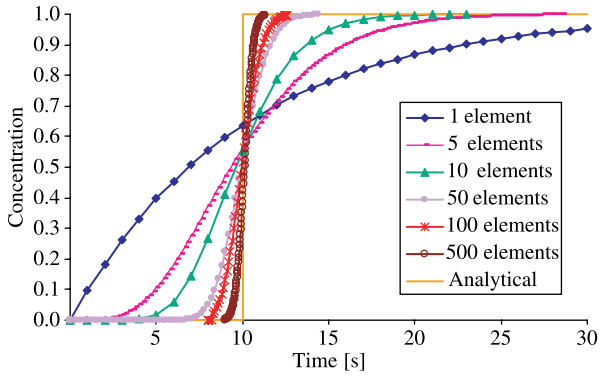

Figure 14. Simulation of the advection front, $Cr = 1.0$ at $x = 10\,\text{mm}$. Available in colour online.

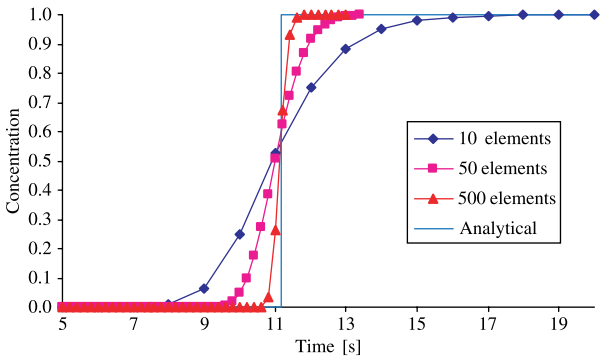

Figure 15. Simulation of the advection front, with $Cr = \exp(-0.02t)$. Available in colour online.

5. Conclusions

In this paper the physical and mechanical moisture-induced damage processes were discussed whereby weakening of the mastic due to moisture diffusion and due to erosion of the mastic caused by high water pressure gradients were identified as important moisture-induced damage processes, which are promoting cohesive failure; and weakening of the aggregate–mastic bond due to continuing moisture diffusion toward this area was identified as an important moisture-induced damage process, leading to an adhesive failure. These equations have been implemented into a new finite element code, named RoAM, which is part of the finite element system CAPA-3D, therefore allowing for comprehensive predictions of pavement material responses under both wet and dry conditions. The developed tool was verified with closed form solutions.

In the next paper, the developed tools are demonstrated in an extensive parametric study and the importance of the various identified fundamental moisture-induced damage parameters on the resulting damage formation are discussed.

Acknowledgements

The authors gratefully acknowledge the financial support of Dr A. de Bondt of Ooms Nederland Holding BV.

References

Atluri, S.N., 2004. *The meshless local-Petrov–Galerkin method for domain and DIE discretization*. Encino: Tech Science Press.

Baptista, A.M., Adams, E.E. and Stolzenback, K.Dd., 1984. The 2-D unsteady transport equation solved by the combined use of the finite element method and the method of characteristics. *Proceedings of the 5th international conference on finite elements in water resources*. New York: Springer-Verlag.

Bear, J., 1972. *Dynamics of fluids in porous media*. New York: Elsevier.

Bear, J. and Bachmat, Y., 1990. *Theory and applications of transport in porous media*. Vol. 4. MA: Kluwer Academic Publishers.

Carslaw, H.S. and Jaeger, J.C., 1959. *Conduction of heat in solids*. Oxford: Clarendon Press.

Casulli, V., 1987. Euler–Lagrangian methods for hyperbolic and convection dominated parabolic problems. In: C. Taylor, D.R.J. Owen, E.E. Hinton, eds. *Computational methods for nonlinear problems*. Swansea: Pineridge.

Casulli, V., 1990. Numerical simulation of shallow water waves. In: G. Gambolati, A. Rinaldo, A. Brebbia, W. Gray, G. Pinder, eds. *Computational methods in surface hydrology*. New York: Springer-Verlag, York.

Cheng, D., Little, D.N., Lytton, R. and Holste, J.C., 2002. Use of surface free energy properties of the asphalt–aggregate system to predict damage potential. *Journal of the association of asphalt paving technologists*, 71, 59–88.

Cheng, D., Little, D.N., Lytton, R. and Holste, J.C., 2003. Moisture damage evaluation of asphalt mixtures by considering both moisture diffusion and repeated—load conditions. *Transportation research record: journal of the transportation research board*, No. 1832, TRB, NRC.

Crank, J., 1975. *The mathematics of diffusion*. 2nd ed. Oxford: Oxford Science Publication.

Dong, W. and Selvadurai, A.P.S., 2006. A Taylor-Galerkin approach for modelling a spherically symetric advective-dispersive transport problem. *Communication in numerical methods in engineering*, 24, 49–63.

Douglas, J. and Russel, T., 1982. Numerical methods for convection dominated diffusion problems based on combining the method of characteristics with finite element of finite difference procedures. *SIAM journal on numerical analyses*, 19, 871–885.

Fick, A., 1855. On liquid diffusion. *Philosophical magazine and journal of science*, 10, 30–39.

Fwa, T.F. and Ong, B.K., 1994. Effect of moisture in aggregates on performance of asphalt mixtures. *Transportation research record: journal of the transportation research board*, 1454, NRC.

Ganzha, V.G. and Vorozhtsov, E.V., 1998. *Computer aided analysis of difference schemes for partial differential equations*. New York: Wiley.

Huber, G., 2005. Tenderness caused by moisture. *Proceedings of the international workshop on moisture-induced damage of asphaltic mixes*, ISBN-13: 978-90-816396-1-1.

Kandhal, P., 1992. *Moisture susceptibility of HMA mixes: identification of problem and recommended solutions*, NCAT Report 92–1.

Kandhal, P., 1994. Field and lab investigation of stripping in asphalt pavements: state-of-the-art. *Transportation research record: journal of the transportation research board*, 1454, NRC.

Kiggundu, B.M. and Roberts, F.L., 1988. Stripping in HMA mixtures: state-of-the-art and critical review of test methods, NCAT Report 88-2.

Kinzelbach, W., 1987. Methods for the simulation of polutant transport in groundwater. *Proceedings of the conference on solving groundwater problems with models*, Colorado.

Kringos, N., 2007. Modelling of combined physical–mechanical moisture-induced damage in asphaltic mixes, PhD dissertation, TU Delft, 2007, ISBN 9789090217659.

Kringos, N. and Scarpas, A., 2005. Simulation of combined mechanical–moisture-induced damage in asphaltic mixes. *Proceedings of the international workshop on moisture-induced damage of asphaltic mixes*, ISBN-13: 978-90-816396-1-1.

Kringos, N. and Scarpas, A., 2005. Raveling of asphaltic mixes: computational identification of controlling parameters. *Transportation research record: journal of the transportation research board*, No. 1929, 79–87.

Kringos, N. and Scarpas, A., 2005. Simulation of combined mechanical-moisture-induced damage in asphaltic mixes. *Proceedings of the international workshop on moisture-induced damage of asphaltic mixes*, Delft.

LeVeque, R.J., 1992. *Numerical methods for conservation laws*. Basel: Birkhauser Verlag.

Lobo Ferreira, J., 1987. A comparative analysis of mathematical mass transport codes for groundwater pollution studies. *Groundwater flow and quality modelling*.

Lytton, R., July 2002. Mechanics and measurement of moisture damage. *Proceedings of moisture damage symposium*, WRI, Wyoming.

Masad, E., Lytton, R. and Little, D., 2005. Moisture-induced damage in asphaltic mixes. *Proceedings of the international workshop on moisture-induced damage of asphaltic mixes*, ISBN-13: 978-90-816396-1-1.

Morton, K.W., 1996. *Numerical solutions of convection–diffusion problems*. London: Chapman and Hall.

Neuman, S.P., 1981. A Eulerian–Lagrangian numerical scheme for the dispersion–convection equation using conjugate space–time grids. *Journal of computational physics*, 41, 270–294.

Quarteroni, A. and Valli, A., 1997. *Numerical approximations of partial differential equations*. Berlin: Springer.

Rice, J.M., 1958. Relationship of aggregate characteristics to the effect of water on bituminous paving mixtures. ASTM STP No. 240.

Scarpas, A., 2000. *CAPA-3D finite element system users manual I, II and III*. Delft: Delft University of Technology Publication.

Scarpas, A., 2005. *A mechanics based computational platform for pavement engineering*, ISBN 90-9019040-6.

Selvadurai, A.P.S., 2000. *Partial differential equations in mechanics*. Vol. 1 & 2. Berlin: Springer-Verlag.

Selvadurai, A.P.S. and Dong, W., 2006a. A Time adaptive scheme for the solution of the advective equation in the presence of a transient flow velocity. *Computer modeling in engineering and science*, 12, 41–54.

Selvadurai, A.P.S. and Dong, W., 2006b. The numerical modelling of advective transport in the presence of fluid pressure transients. *International journal for numerical and analytical methods in geomechanics*, 30, 615–634.

Stuart, K., 1990. *Moisture damage in asphalt mixtures-state-of-the-art*, Report FHWA-RD-90-019, FHWA, VA 22101-2296.

Taylor, M.A. and Khosla, N.P., 1983. Stripping of asphalt pavements: state-of-the-art. *Transportation research record: journal of the transportation research board*, 911, 150–157.

Thunqvist, E.L., 2001. Long term effects of deicing salt on the roadside environment part II: groundwater and surface water. *Proceedings of the 9th maintenance management conference,* Alaska.

Wang, Y. and Hutter, K., 2001. Comparisons of numerical methods with respect to convectively dominated problems. *International journal for numerical methods in fluids*, 37, 721–745.